

BIFURCATIONS AND HYDRA EFFECTS IN A REACTION-DIFFUSION PREDATOR-PREY MODEL WITH HOLLING II FUNCTIONAL RESPONSE

Hongyu Chen¹ and Chunrui Zhang^{1,†}

Abstract In this paper, through bifurcation analysis and numerical simulations, we consider a reaction-diffusion predator-prey model with Holling II functional response to analyze the existence of hydra effect and the relationship between mortality independent of predator density and different steady-state solutions of the system. The hydra effect, which is a paradoxical result in both theoretical and applied ecology, refers to the phenomenon in which an increase in population mortality enhances its own population size. We investigate the existence of the hydra effect when the positive equilibrium point is locally asymptotically stable and Turing unstable. Meanwhile, numerical simulations verify the existence of the hydra effect when the one-dimensional reaction-diffusion system has a spatially inhomogeneous steady-state solution. In addition, we introduce the existence of the Turing bifurcation, the Hopf bifurcation, and the Turing-Hopf bifurcation with the parameters d_2 and m_C , respectively, as well as the normal form for the Turing-Hopf bifurcation. Based on the obtained normal form, we analyze the complex spatio-temporal dynamics near the Turing-Hopf bifurcation point. Finally, the numerical simulations are carried out to corroborate the obtained theoretical results.

Keywords Predator-prey system, hydra effect, Turing instability, Turing-Hopf bifurcation, normal form.

MSC(2010) 34C23, 35K57.

1. Introduction

All living things are not immune to death. Old age, disease, predation and natural disasters all lead to the death of organisms. It is commonly understood that population density decreases as mortality increases [7, 16, 17, 19–22, 26–28, 30]. However, there are phenomena in nature that are contrary to this [23, 24]. The hydra effect is defined as the phenomenon in which when the mortality rate of a population increases, its equilibrium density or time-averaged density also increases [4, 8, 13, 25]. Ricker first identified such paradoxical phenomenon in a single-species homogeneous discrete model discovery and showed that this phenomenon may be of interest in pest control [11]. However, for a long time, his ideas were largely ignored [18].

[†]The corresponding author. Email: math@nefu.edu.cn(C. Zhang)

¹Department of Mathematics, Northeast Forestry University, 150040, Harbin, China

This idea became popular as more and more articles on the subject appeared [2, 14]. Nowadays, it has been widely recognized that the hydra effect is of great importance in applied ecology and epidemiology [4, 5, 29]. Therefore, the study of the hydra effect has become a hot topic in theoretical ecology and is well worth studying.

Abrams and Quince were pioneers in the study of the hydra effect in stage-structured predator-prey systems [1]. As the understanding of the hydra effect in population dynamics has advanced, there is some evidence for a hydra effect in situations where species coexist in an oscillatory form. Sieber and Hilker [18, 25] studied Gaussian predator-prey systems with Holling II and III functional responses and concluded that the time-averaged density of predators increases with mortality when the predator-prey community evolves in a cyclic pattern. Later, the mathematical conditions for the emergence of the hydra effect at steady state for unstructured population models were provided by Cortez and Abrams [3, 6]. And they also found the presence of the hydra effect in different predator-prey systems.

The previously mentioned theoretical studies are limited to cases of spatial homogenization, ignoring mechanisms such as species dispersal and migration. DeAngelis and Yurek [12] noted that spatially explicit models in ecology are increasingly being studied by researchers using different methods. The researchers, Cortez and Abrams [6] and Costa and dos Anjos [9], established the hydra effect in a planar predator-prey system with highly nonlinear terms. In Chen and Zhang [10], an example of the presence of the hydra effect in a reaction-diffusion predator-prey system when a spatially inhomogeneous steady-state solution occurs was given by numerical simulations. It is very complicated to analyze these models. Therefore, so far, there have been few studies of hydra effects in spatially explicit models that consider diffusion. Recently, Lucas dos Anjos [4] presented some examples of the existence of the hydra effect in population models, including continuous-time population models and discrete-time population models. These models are described by nonlinear systems of ordinary differential equations and difference equations, respectively. Through numerical simulations, they found that there is a hydra effect in the static dynamics of some one-dimensional predator-prey models. The model they studied is described by a system of nonlinear partial differential equations with different functional response functions. They found that an increase in response diffusivity for the Holling II functional response shortens the range of the hydra effect. Their main model studied is as follows:

$$\begin{cases} \frac{\partial R}{\partial t} = D_R \frac{\partial^2 R}{\partial x^2} + rR \left(1 - \frac{R}{K}\right) - \frac{a_{CR}RC}{1 + a_{CR}Th_{CR}R}, \\ \frac{\partial C}{\partial t} = D_C \frac{\partial^2 C}{\partial x^2} + \frac{ef_{RC}a_{CR}RC}{1 + a_{CR}Th_{CR}R} - m_C C - q_C C^2, \end{cases} \quad (1.1)$$

where R and C are the densities of prey and predator, respectively. r and K are the inherent growth rate and the environmental capacity of prey R , respectively. m_C and q_C are the per capita mortality rates of density-independent and density-related species C , respectively. D_R and D_C are the diffusion coefficients of species R and C respectively, and ef_{RC} is the conversion factor of species R to species C . a_{CR} and Th_{CR} are the coefficient of attack and time of effect of species C on species R , respectively. All parameters are positive constants.

We consider the study by Lucas dos Anjos et al. [4] to be very interesting. However, in their paper, they mainly used numerical simulations to demonstrate the existence of the hydra effect and did not conduct any theoretical analysis or

specific study on how mortality affects population size. On the basis of their study, we would like to use their model to conduct a theoretical analysis with mortality m_C as a parameter, and believe that many interesting conclusions will be obtained. We denote as $\alpha = \frac{ef_{RC}}{m_C}$, $\beta = \frac{q_C}{m_C}$, system (1.1) can be rewritten as

$$\begin{cases} \frac{\partial u(x,t)}{\partial t} = d_1 \frac{\partial^2 u}{\partial x^2} + ru(1 - \frac{u}{K}) - \frac{a_{CR}uv}{1 + a_{CR}Th_{CR}u}, & x \in \Omega, t > 0, \\ \frac{\partial v(x,t)}{\partial t} = d_2 \frac{\partial^2 v}{\partial x^2} + m_C v (\frac{\alpha a_{CR}u}{1 + a_{CR}Th_{CR}u} - 1 - \beta v), & x \in \Omega, t > 0, \\ u_x(x,t) = v_x(x,t) = 0, & x \in \partial\Omega, t > 0, \\ u(x,0) = u_0(x) \geq 0, v(x,0) = v_0(x) \geq 0, & x \in \bar{\Omega}. \end{cases} \quad (1.2)$$

In this paper, we investigate the occurrence of the hydra effect when the positive equilibrium point is locally asymptotically stable and Turing unstable through bifurcation analysis and numerical simulations of a one-dimensional spatial predator-prey model with Holling II functional response. We also investigate how small perturbations in per capita mortality for species C resulted in different steady states for predator and prey populations. Essentially, the purpose of this study is to analyze how mortality m_C affects the equilibrium state of predator and prey populations. Because the hydra effect refers to the increase in the mean density or stable population of a species with increasing mortality, it is necessary to examine in detail the effect of changes in mortality m_C on population size.

The organizational structure of this paper is as follows. In Section 2, the existence and stability conditions for all feasible equilibrium points of the system (1.2) are analysed. Furthermore, the bifurcation analysis is investigated in Section 3, where the existence of the Turing bifurcation, the Hopf bifurcation and the Turing-Hopf bifurcation are shown by choosing the d_2 and m_C as bifurcation parameters, respectively. In addition, we investigate the presence of the hydra effect when the positive equilibrium point is locally asymptotically stable and Turing unstable. Moreover, the normal form of the Turing-Hopf bifurcation for the system (1.2) near the unique positive constant equilibrium is obtained in Section 4. And finally, in Section 5, numerical simulations are carried out to verify the obtained theoretical conclusions.

2. Existence and stability of equilibrium points

In this section, the existence of coexistence equilibrium of the system (1.2) is analyzed. Considering the following equation

$$\begin{cases} f(u,v) = ru(1 - \frac{u}{K}) - \frac{a_{CR}uv}{1 + a_{CR}Th_{CR}u} = 0, \\ g(u,v) = m_C v (\frac{\alpha a_{CR}u}{1 + a_{CR}Th_{CR}u} - 1 - \beta v) = 0. \end{cases} \quad (2.1)$$

The system (1.2) has three meaningful equilibrium points, and their feasibility and stability are given below.

Theorem 2.1. *The trivial equilibrium point $E_0(0,0)$ always exists and is a saddle point.*

Proof. $J(E_0) = \begin{pmatrix} r & 0 \\ 0 & -m_C \end{pmatrix}$ is the Jacobian matrix of system (1.2) around E_0 and $\lambda_1 = r > 0$ and $\lambda_2 = -m_C < 0$ are the eigenvalues. So, E_0 is a saddle point. \square

Theorem 2.2. *The prey only equilibrium point $E_1(K, 0)$ always exists ($\because K > 0$) and is locally asymptotically stable when $-1 + Ka_{CR}(\alpha - Th_{CR}) < 0$, non-hyperbolic when $-1 + Ka_{CR}(\alpha - Th_{CR}) = 0$ and unstable when $-1 + Ka_{CR}(\alpha - Th_{CR}) > 0$.*

Proof. $E_1(K, 0)$ is a prey-only equilibrium, which means that at this equilibrium point there is only prey and the population density of predators is zero. $J(E_1) = \begin{pmatrix} -r & -\frac{Ka_{CR}}{1+Ka_{CR}Th_{CR}} \\ 0 & \frac{m_C(-1+Ka_{CR}(\alpha-Th_{CR}))}{1+Ka_{CR}Th_{CR}} \end{pmatrix}$ is the Jacobian matrix of system (1.2) around E_1 and the eigenvalues are $\lambda_1 = -r < 0$ and $\lambda_2 = \frac{m_C(-1+Ka_{CR}(\alpha-Th_{CR}))}{1+Ka_{CR}Th_{CR}}$. Therefore, when λ_2 takes different signs, the E_1 has different stable states. When $\lambda_2 < 0$, E_1 is locally asymptotically stable; when $\lambda_2 = 0$, E_1 is non-hyperbolic; when $\lambda_2 > 0$, E_1 is unstable. \square

Theorem 2.3. *Assume that $u_*a_{CR}(\alpha - Th_{CR}) > 1$ holds, then there exists at least one positive equilibrium point $E_*(u_*, v_*)$ for system (1.2).*

Proof. By using the second equation of (2.1), we are able to obtain

$$v = \frac{-1 + u\alpha a_{CR} - ua_{CR}Th_{CR}}{\beta(1 + ua_{CR}Th_{CR})}. \tag{2.2}$$

Substituting (2.2) into the first equation of (2.1), we obtain the following expression

$$\begin{aligned} h(u) = & -r\beta a_{CR}^2 Th_{CR}^2 u^3 \\ & + (-2r\beta a_{CR}Th_{CR} + Kr\beta a_{CR}^2 Th_{CR}^2)u^2 \\ & + (-r\beta - K\alpha a_{CR}^2 + 2Kr\beta a_{CR}Th_{CR} + Ka_{CR}^2 Th_{CR})u + Kr\beta + Ka_{CR}. \end{aligned}$$

Obviously, $h(0) = Kr\beta + Ka_{CR} > 0$ and $\lim_{u \rightarrow +\infty} h(u) \rightarrow -\infty$, then there exists at least one positive constant u_* satisfying $h(u_*) = 0$, and at this point $v_* = \frac{-1 + u_*\alpha a_{CR} - u_*a_{CR}Th_{CR}}{\beta(1 + u_*a_{CR}Th_{CR})}$. If $v_* > 0$, it means that the system (1.2) has at least one positive equilibrium point (u_*, v_*) . \square

In this article, we mainly study the relevant properties of the coexistence equilibrium of the system (1.2). The Theorem 2.3 means that the system (1.2) has at least one positive equilibrium point. We suppose that $E_*(u_*, v_*)$ is the positive equilibrium point of the system (1.2) for the remainder of the article.

3. Bifurcation analysis and hydra effect

3.1. Linear stability analysis and hydra effect

Firstly, we conduct a linear stability analysis of the system (1.2). Define a real-valued Sobolev space

$$X := \{(u, v) \in [H^2(0, l\pi)]^2 : (u_x, v_x)|_{x=0, l\pi} = 0\},$$

and the complexification of X to be

$$X_c := X \oplus iX = \{x_1 + ix_2 : x_1, x_2 \in X\}.$$

Then the system (1.2) can be written in the following abstract form in space X

$$\begin{pmatrix} u_t \\ v_t \end{pmatrix} = D \begin{pmatrix} \Delta u \\ \Delta v \end{pmatrix} + L \begin{pmatrix} u \\ v \end{pmatrix},$$

where

$$D = \begin{pmatrix} d_1 & 0 \\ 0 & d_2 \end{pmatrix}, L = \begin{pmatrix} a_1 & a_2 \\ m_C b_1 & m_C b_2 \end{pmatrix},$$

and

$$\begin{aligned} a_1 &= \frac{r(K - 2u_*) + r(K - 2u_*)u_*^2 a_{CR}^2 Th_{CR}^2 - a_{CR}(Kv_* + 2ru_*(-K + 2u_*)Th_{CR})}{K(1 + u_* a_{CR} Th_{CR})^2}, \\ a_2 &= -\frac{u_* a_{CR}}{1 + u_* a_{CR} Th_{CR}}, \\ b_1 &= \frac{v_* \alpha a_{CR}}{(1 + u_* a_{CR} Th_{CR})^2}, \\ b_2 &= \frac{-1 - 2v_* \beta + u_* a_{CR}(\alpha - (1 + 2v_* \beta)Th_{CR})}{1 + u_* a_{CR} Th_{CR}}. \end{aligned}$$

It can be seen from the literature [15],

$$-\varphi_{xx} = \mu\varphi, x \in (0, l\pi), \varphi_x|_{x=0, l\pi} = 0,$$

and the characteristic value of it is $\mu_n = \frac{n^2}{l^2}, n \in N_0 := \{0, 1, 2, \dots\}$. The corresponding characteristic function is $\varphi_n(x) = \cos \frac{n}{l}x$. Let

$$\begin{pmatrix} \phi \\ \varphi \end{pmatrix} = \sum_{n=0}^{\infty} \begin{pmatrix} a_n \\ b_n \end{pmatrix} \cos \frac{n}{l}x$$

be the characteristic function of $L + \Delta$ corresponding to the characteristic value λ . Then we can obtain

$$L_n \begin{pmatrix} \phi \\ \varphi \end{pmatrix} = \lambda \begin{pmatrix} \phi \\ \varphi \end{pmatrix}, n \in N_0,$$

where

$$L_n = \begin{pmatrix} a_1 - d_1 \frac{n^2}{l^2} & a_2 \\ m_C b_1 & m_C b_2 - d_2 \frac{n^2}{l^2} \end{pmatrix}.$$

It can be seen that the eigenvalue of $L + \Delta$ can be given by the eigenvalue of L_n , with $n \in N_0$. Then at the positive equilibrium point $E_*(u_*, v_*)$, we can obtain the following characteristic equation, that is

$$\lambda^2 - TR_n \lambda + DET_n = 0, n \in N_0, \quad (3.1)$$

where

$$\begin{cases} \mu_n = \frac{n^2}{l^2}, \\ TR_n = -(d_1 + d_2)\mu_n + a_1 + b_2m_C, \\ DET_n = d_1d_2\mu_n^2 - (a_1d_2 + b_2d_1m_C)\mu_n + (a_1b_2 - a_2b_1)m_C, \end{cases} \tag{3.2}$$

and the eigenvalues of the system (1.2) are given by

$$\lambda_{1,2}^{(n)} = \frac{TR_n \pm \sqrt{TR_n^2 - 4DET_n}}{2}, n \in N_0. \tag{3.3}$$

Then we make the following hypotheses:

- (A₁) $a_1 + b_2m_C < 0$.
- (A₂) $a_1b_2 - a_2b_1 > 0$.

If the assumptions (A₁) and (A₂) are both valid, then when $n = 0$, there is $TR_0 < 0$ and $DET_0 > 0$. That is to say, the real parts of the eigenvalues of the system (1.2) are all less than zero. Therefore, the following theorem is obtained.

Theorem 3.1. *Suppose that (A₁) and (A₂) hold. Then the ordinary differential equation system corresponding to the system (1.2) is locally asymptotically stable at the positive equilibrium point $E_*(u_*, v_*)$.*

We want to verify whether the per capita mortality of species C can induce hydra effects in the stable equilibrium of the model. The mathematical conditions for the emergence of the hydra effect at steady state for unstructured population models were provided by Cortez and Abrams [6]. Next, these conditions are used to study our model. The coexistence equilibrium $E_*(u_*, v_*)$ satisfies

$$\begin{aligned} ru_*(1 - \frac{u_*}{K}) - \frac{a_C R u_* v_*}{1 + a_C R T h_C R u_*} &= 0, \\ \frac{e f_{RC} a_C R u_* v_*}{1 + a_C R T h_C R u_*} - m_C v_* - q_C v_*^2 &= 0. \end{aligned} \tag{3.4}$$

In the Jacobian matrix, both a_2 and b_1 have a certain sign, i.e., $a_2 < 0$, $b_1 > 0$. However, a_1 and b_2 can change their signs on different parameter spaces. Assume that the positive equilibrium point $E_*(u_*, v_*)$ is locally asymptotically stable even when $a_1 > 0$. We then calculate the change in predator species stock with mortality by differentiating m_C in the system (3.4). We can obtain

$$\begin{aligned} a_1 \frac{du_*}{dm_C} + a_2 \frac{dv_*}{dm_C} &= 0, \\ m_C b_1 \frac{du_*}{dm_C} + m_C b_2 \frac{dv_*}{dm_C} &= v_*. \end{aligned} \tag{3.5}$$

Applying Cramer’s rule to the solution of the system (3.5), we can obtain

$$\frac{du_*}{dm_C} = \frac{-a_2 v_*}{(a_1 b_2 - a_2 b_1) m_C}, \frac{dv_*}{dm_C} = \frac{a_1 v_*}{(a_1 b_2 - a_2 b_1) m_C}.$$

If the positive equilibrium $E_*(u_*, v_*)$ is locally asymptotically stable, i.e., (A_1) and (A_2) hold, and $a_1 > 0$, then we obtain

$$\frac{du_*}{dm_C} > 0, \frac{dv_*}{dm_C} > 0.$$

Thus, it is known that in the steady state, the number of both predator and prey populations increases with the increase in mortality m_C . Moreover, in the steady state, the number of prey populations always increases (i.e., there is no need to restrict $a_1 > 0$). Figure 1 verifies our idea. Also, we can obtain the following theorem.

Theorem 3.2. *Predator species experiences hydra effects at stable states, when $a_1 > 0$.*

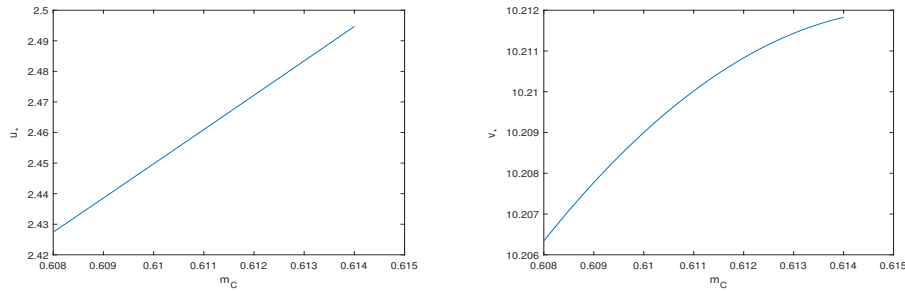


Figure 1. The existence of the hydra effect is depicted when the system is in a stable state. The parameters value are $r = 5.01$, $K = 6.01$, $a_{CR} = 1.01$, $Th_{CR} = 1$, $ef_{RC} = 1$, $q_C = 0.01$.

3.2. Turing instability and hydra effect

In this section, the existence conditions of the Turing instability are analyzed. Under the assumptions that (A_1) and (A_2) are established, it is known from Theorem 3.1 that there is $TR_n < TR_0 < 0$ for $n \in N_0$. Then when $DET_n(d_2) = d_1 d_2 \mu_n^2 - (a_1 d_2 + b_2 d_1 m_C) \mu_n + (a_1 b_2 - a_2 b_1) m_C$, d_2 is selected as the Turing bifurcation line parameter. Let $a_1 > 0$ and discuss in the following three situations:

Situation 1. $d_2 \leq -\frac{b_2 d_1 m_C}{a_1}$,

Situation 2. $d_2 > -\frac{b_2 d_1 m_C}{a_1}$, and $\Delta < 0$,

Situation 3. $d_2 > -\frac{b_2 d_1 m_C}{a_1}$, and $\Delta > 0$,

where $\Delta = (a_1 d_2 + b_2 d_1 m_C)^2 - 4d_1 d_2 (a_1 b_2 - a_2 b_1) m_C$. After the analysis and discussion of the above three situations, we can get the following theorem.

Theorem 3.3. *Suppose (A_1) and (A_2) hold. The positive equilibrium $E_*(u_*, v_*)$ for the system (1.2) is locally asymptotically stable in Situation 1 or Situation 2. In addition, in Situation 3, if there is no $\mu_n (n \in N_0)$ satisfying $DET_n < 0$, the positive equilibrium point $E_*(u_*, v_*)$ for the system (1.2) is locally asymptotically stable. However, in Situation 3, if there exists at least one $\mu_n (n \in N_0)$ satisfying $DET_n < 0$, $E_*(u_*, v_*)$ is Turing unstable.*

Proof. Suppose that (A_1) and (A_2) hold. Under the condition that the parameters of Situation 1 or Situation 2 are satisfied, there is $TR_n < TR_0 < 0$ for $n \in N_0$, then if $DET_n > 0 (n \in N_0)$, the system (1.2) has the eigenvalue of the negative real part. When the parameter relationship belongs to Situation 3, and there is not $n \in N_0$ such that $DET_n < 0$, then a similar method can be used to prove the conclusion. When the parameter relationship belongs to Situation 3, and there is a $n^1 \in N_0$ such that $DET_{n^1} < 0$, then the real part of the eigenvalue $\lambda_1^{(n^1)} = \frac{TR_{n^1} + \sqrt{TR_{n^1}^2 - 4DET_{n^1}}}{2}$ of the system (1.2) will be positive, which means that the positive equilibrium point $E_*(u_*, v_*)$ of the system (1.2) becomes no longer stable. The proof of the theorem is complete. \square

As stated in Chen and Zhang [10], we also found the example of the presence of the hydra effect when Turing instability occurs, as shown in Figure 2.

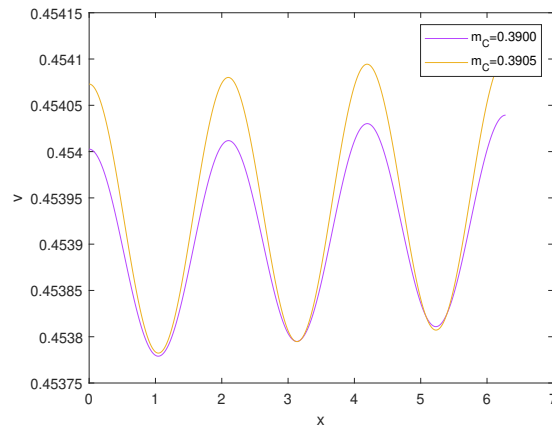


Figure 2. Spatial distribution of predator population size when the other parameters are fixed at values: $d_1 = 0.01, d_2 = 2.51, r = 0.25, K = 14.95, a_{CR} = 1.01, Th_{CR} = 1, \alpha = 2.61, \beta = 0.61, l = 1, x \in (0, 2\pi)$ and the predator per capita mortality rate m_C is taken to be 0.3900 and 0.3905, respectively.

3.3. Hopf bifurcation

In this section, the existence conditions of the Hopf bifurcation are analyzed. Denote

$$m_C = m_C^n = \frac{(d_1 + d_2)\mu_n - a_1}{b_2} > 0, n \in N_0. \tag{3.6}$$

Obviously, $DET_0(m_C^0) = (a_1b_2 - a_2b_1)m_C^0 > 0$ under hypothesis (A_2) . Denote

$$\Lambda = \{n \in N_0 | DET_n > 0 \text{ and } m_C^n > 0\}. \tag{3.7}$$

After analysis, we can get the following theorem.

Theorem 3.4. *If (A_2) holds, the system (1.2) undergoes a Hopf bifurcation at the positive equilibrium point $E_*(u_*, v_*)$ when $m_C = m_C^n$, for $n \in \Lambda$. Moreover, the bifurcating periodic solution is spatially homogeneous when $m_C = m_C^0$ and spatially nonhomogeneous when $m_C = m_C^n$ for $n \in \Lambda$ and $n \neq 0$.*

Proof. Let $\lambda_n(m_C^n) = \alpha_n(m_C^n) \pm i\eta_n(m_C^n)$, $n \in \Lambda$, be the roots of Eq.(3.1).

(i) When $m_C = m_C^n$, we can get $TR_n(m_C) = 0$ and $DET_n(m_C) > 0$ for $n \in \Lambda$. Then $\lambda_n(m_C^n) = \pm i\sqrt{DET_n(m_C^n)}$ is a pair of pure imaginary roots of the characteristic equation (3.1) for system (1.2).

(ii) When m_C is near m_C^n , from Eq.(3.3), we can get

$$\alpha_n(m_C) \pm i\eta_n(m_C) = \frac{TR_n(m_C) \pm \sqrt{TR_n^2(m_C) - 4DET_n(m_C)}}{2}.$$

Then we can obtain $\frac{d\alpha_n(m_C)}{dm_C} = \frac{b_2}{2} < 0$. That is to say, for each m_C^n , $n \in \Lambda$, the transversal condition holds. This completes the proof. \square

3.4. Turing-Hopf bifurcation

In this section, the existence conditions of the Turing-Hopf bifurcation are analyzed. For the system (1.2) to undergo a Turing-Hopf bifurcation, the following conditions need to be satisfied:

(i) When $n = 0$, the characteristic equation (3.1) for system (1.2) has a pair of pure imaginary roots $\pm i\omega$. This phenomenon can be produced when $m_C = m_C^0 = -\frac{a_1}{b_2}$.

(ii) When $n > 0$, the characteristic equation (3.1) for system (1.2) has a single zero root. This phenomenon can be produced when $DET_n = 0$.

In this section, we assume (A_2) always holds. Denote

$$d_2^n = m_C \left(\frac{b_2 d_1 \mu_n + (a_2 b_1 - a_1 b_2)}{\mu_n(-a_1 + d_1 \mu_n)} \right), S = \{n \in N, a_1 - d_1 \mu_n > 0\},$$

such that

$$d_2^{n_*} = m_C^* \left(\frac{b_2 d_1 \mu_{n_*} + (a_2 b_1 - a_1 b_2)}{\mu_{n_*}(-a_1 + d_1 \mu_{n_*})} \right) = \min_{n \in S} m_C^* \left(\frac{b_2 d_1 \mu_n + (a_2 b_1 - a_1 b_2)}{\mu_n(-a_1 + d_1 \mu_n)} \right).$$

From the Theorem 3.4, we can know that the system (1.2) will have a Hopf bifurcation at the positive equilibrium point $E_*(u_*, v_*)$, when $m_C = m_C^0 = -\frac{a_1}{b_2}$. Therefore, $m_C^* = -\frac{a_1}{b_2}$, when $n = n_*$. d_2^n are the Turing bifurcation lines and m_C^* is the Hopf bifurcation line. When $n = n_*$, we hope to find the first intersection of these two types of bifurcation lines in the first quadrant, which is the Turing-Hopf bifurcation point. After the above analysis, we can get the following theorem.

Theorem 3.5. *If the hypothesis (A_2) holds, the following conclusions can be drawn:*

- (i) *If $S = \emptyset$, the Turing-Hopf bifurcation does not be undergone for the system (1.2);*
- (ii) *If $S \neq \emptyset$, the system (1.2) undergoes Turing-Hopf bifurcation at the point $(m_C, d_2) = (m_C^*, d_2^{n_*})$, and the positive equilibrium $E_*(u_*, v_*)$ of the system (1.2) is locally asymptotically stable for*

$$(m_C, d_2) \in \left\{ (m_C, d_2) \mid m_C > m_C^*, 0 < d_2 < m_C \left(\frac{b_2 d_1 \mu_{n_*} + (a_2 b_1 - a_1 b_2)}{\mu_{n_*}(-a_1 + d_1 \mu_{n_*})} \right) \right\}.$$

Proof. In $m_C - d_2$ plane, we define the Turing bifurcation curves as follows:

$$\mathcal{L}_n : d_2^n = m_C \left(\frac{b_2 d_1 \mu_n + (a_2 b_1 - a_1 b_2)}{\mu_n(-a_1 + d_1 \mu_n)} \right), n \in S.$$

The Hopf bifurcation curve is $\mathcal{H}_0 : m_C = m_C^*$.

(i) If $S = \emptyset$, then there is no intersection point between Turing bifurcation curves \mathcal{L}_n and the Hopf bifurcation curve \mathcal{H}_0 in the first quadrant. This indicates that the system (1.2) does not undergo Turing-Hopf bifurcation.

(ii) If $S \neq \emptyset$, then the Turing bifurcation curve \mathcal{L}_{n_*} and the Hopf bifurcation curve \mathcal{H}_0 intersect at point $(m_C^*, d_2^{n_*})$. This point is called the Turing-Hopf bifurcation point. In addition, when

$$(m_C, d_2) \in \left\{ (m_C, d_2) \mid m_C > m_C^*, 0 < d_2 < m_C \left(\frac{b_2 d_1 \mu_{n_*} + (a_2 b_1 - a_1 b_2)}{\mu_{n_*} (-a_1 + d_1 \mu_{n_*})} \right) \right\},$$

it is easy to prove that $TR_n < 0$ and $DET_n > 0$ for $n \in N_0$. Then the positive equilibrium point $E_*(u_*, v_*)$ is locally asymptotically stable. Next, let us verify the transversality conditions. Suppose $\lambda_1(m_C, d_2) = \alpha_1(m_C, d_2) + i\eta_1(m_C, d_2)$ with $\alpha_1(m_C^*) = 0, \eta_1(m_C^*) = \omega > 0$ when $n = 0$, and $\lambda_2(m_C, d_2) = \alpha_2(m_C, d_2) + i\eta_2(m_C, d_2)$ with $\alpha_2(m_C^*, d_2^{n_*}) = 0, \eta_2(m_C^*, d_2^{n_*}) = 0$ when $n = n_* > 0$, then the following transversality conditions can be obtained:

$$\begin{aligned} \left. \frac{dRe(\lambda_1(m_C, d_2))}{dm_C} \right|_{m_C = m_C^*, \mathcal{H}_0} &= \frac{b_2}{2} < 0, \\ \left. \frac{dRe(\lambda_2(m_C, d_2))}{dm_C} \right|_{m_C = m_C^*, \mathcal{L}_{n_*}} &= \frac{-b_2 d_1 \mu_{n_*} + a_1 b_2 - a_2 b_1}{TR_{n_*}} < 0. \end{aligned}$$

This completes the proof. □

4. Normal forms for Turing-Hopf bifurcation

In this section, the normal form for the Turing-Hopf bifurcation of the reaction-diffusion system (1.2) under the positive equilibrium point $E_*(u_*, v_*)$ is computed. Firstly, we introduce the parameters σ_1 and σ_2 by letting $m_C = m_C^* + \sigma_1$ and $d_2 = d_2^{n_*} + \sigma_2$, which satisfy that the reaction-diffusion system (1.2) will undergo Turing-Hopf bifurcation at the positive equilibrium point $E_*(u_*, v_*)$, when $\sigma_1 = 0$ and $\sigma_2 = 0$. Then the system (1.2) can be transformed into

$$\begin{cases} \frac{\partial u}{\partial t} = d_1 \frac{\partial^2 u}{\partial x^2} + ru(1 - \frac{u}{K}) - \frac{a_{CR}uv}{1 + a_{CR}Th_{CR}u}, \\ \frac{\partial v}{\partial t} = (d_2^{n_*} + \sigma_2) \frac{\partial^2 v}{\partial x^2} + (m_C^* + \sigma_1)v \left(\frac{\alpha a_{CR}u}{1 + a_{CR}Th_{CR}u} - 1 - \beta v \right). \end{cases} \tag{4.1}$$

For the system (4.1), $E_*(u_*, v_*)$ is still the positive equilibrium point. By making the transformations $\bar{u} = u - u_*$ and $\bar{v} = v - v_*$ to move $E_*(u_*, v_*)$ to the origin. After omitting the horizontal bar, the system (4.1) becomes

$$\begin{cases} \frac{\partial u}{\partial t} = d_1 \frac{\partial^2 u}{\partial x^2} + r(u + u_*) \left(1 - \frac{u + u_*}{K} \right) - \frac{a_{CR}(u + u_*)(v + v_*)}{1 + a_{CR}Th_{CR}(u + u_*)}, \\ \frac{\partial v}{\partial t} = (d_2^{n_*} + \sigma_2) \frac{\partial^2 v}{\partial x^2} + (m_C^* + \sigma_1)(v + v_*) \left(\frac{\alpha a_{CR}(u + u_*)}{1 + a_{CR}Th_{CR}(u + u_*)} - 1 - \beta(v + v_*) \right). \end{cases} \tag{4.2}$$

Then according to [15], for the system (4.2), we can get

$$D(\sigma) = \begin{pmatrix} d_1 & 0 \\ 0 & d_2^{m_*} + \sigma_2 \end{pmatrix},$$

$$L(\sigma) = \begin{pmatrix} a_1 & a_2 \\ (m_C^* + \sigma_1)b_1 & (m_C^* + \sigma_1)b_2 \end{pmatrix},$$

$$F(\phi, \sigma) = \begin{pmatrix} r(\phi_1 + u_*)\left(1 - \frac{\phi_1 + u_*}{K}\right) - \frac{a_{CR}(\phi_1 + u_*)(\phi_2 + v_*)}{1 + a_{CR}Th_{CR}(\phi_1 + u_*)} - a_1\phi_1 - a_2\phi_2 \\ (m_C^* + \sigma_1)(\phi_2 + v_*)\left(\frac{\alpha a_{CR}(\phi_1 + u_*)}{1 + a_{CR}Th_{CR}(\phi_1 + u_*)} - 1 - \beta(\phi_2 + v_*)\right) \\ -(m_C^* + \sigma_1)b_1\phi_1 - (m_C^* + \sigma_1)b_2\phi_2 \end{pmatrix},$$

where $\phi = (\phi_1, \phi_2)^T \in X$. Then, we can obtain

$$D(0) = \begin{pmatrix} d_1 & 0 \\ 0 & d_2^{m_*} \end{pmatrix}, \quad D_1(\sigma) = \begin{pmatrix} 0 & 0 \\ 0 & 2\sigma_2 \end{pmatrix},$$

$$L(0) = \begin{pmatrix} a_1 & a_2 \\ m_C^*b_1 & m_C^*b_2 \end{pmatrix}, \quad L_1(\sigma) = \begin{pmatrix} 0 & 0 \\ 2b_1\sigma_1 & 2b_2\sigma_1 \end{pmatrix},$$

$$Q(\phi, \psi) = \begin{pmatrix} \alpha_{11}\phi_1\psi_1 + \alpha_{12}(\phi_1\psi_2 + \psi_1\phi_2) + \alpha_{13}\phi_2\psi_2 \\ \alpha_{21}\phi_1\psi_1 + \alpha_{22}(\phi_1\psi_2 + \psi_1\phi_2) + \alpha_{23}\phi_2\psi_2 \end{pmatrix},$$

$$C(\phi, \psi, v) = \begin{pmatrix} \beta_{11}\phi_1\psi_1v_1 + \beta_{12}(\phi_1\psi_1v_2 + \phi_1\psi_2v_1 + \phi_2\psi_1v_1) \\ +\beta_{13}(\phi_1\psi_2v_2 + \phi_2\psi_1v_2 + \phi_2\psi_2v_1) + \beta_{14}\phi_2\psi_2v_2 \\ \beta_{21}\phi_1\psi_1v_1 + \beta_{22}(\phi_1\psi_1v_2 + \phi_1\psi_2v_1 + \phi_2\psi_1v_1) \\ +\beta_{23}(\phi_1\psi_2v_2 + \phi_2\psi_1v_2 + \phi_2\psi_2v_1) + \beta_{24}\phi_2\psi_2v_2 \end{pmatrix},$$

with

$$\alpha_{11} = -\frac{2r}{K} + \frac{2v_*a_{CR}^2Th_{CR}}{(1 + u_*a_{CR}Th_{CR})^3}, \quad \alpha_{12} = -\frac{a_{CR}}{(1 + u_*a_{CR}Th_{CR})^2}, \quad \alpha_{13} = 0,$$

$$\alpha_{21} = -\frac{2v_*\alpha m_C^*a_{CR}^2Th_{CR}}{(1 + u_*a_{CR}Th_{CR})^3}, \quad \alpha_{22} = \frac{\alpha m_C^*a_{CR}}{(1 + u_*a_{CR}Th_{CR})^2}, \quad \alpha_{23} = -2\beta m_C^*,$$

$$\beta_{11} = -\frac{6v_*a_{CR}^3Th_{CR}^2}{(1 + u_*a_{CR}Th_{CR})^4}, \quad \beta_{12} = \frac{2a_{CR}^2Th_{CR}}{(1 + u_*a_{CR}Th_{CR})^3}, \quad \beta_{13} = \beta_{14} = 0,$$

$$\beta_{21} = \frac{6v_*\alpha m_C^*a_{CR}^3Th_{CR}^2}{(1 + u_*a_{CR}Th_{CR})^4}, \quad \beta_{22} = -\frac{2\alpha m_C^*a_{CR}^2Th_{CR}}{(1 + u_*a_{CR}Th_{CR})^3}, \quad \beta_{23} = \beta_{24} = 0,$$

and

$$\phi = (\phi_1, \phi_2)^T, \psi = (\psi_1, \psi_2)^T, v = (v_1, v_2)^T \in X.$$

The characteristic matrix corresponding to the system (4.2) is

$$D_n(\lambda) = \begin{pmatrix} \lambda - a_1 + d_1\mu_n & -a_2 \\ -m_C^*b_1 & \lambda - m_C^*b_2 + d_2^{n*}\mu_n \end{pmatrix}, \quad n \in N.$$

According to the Theorem 3.5, $\lambda = \pm i\omega$ with $\omega = \sqrt{(a_1b_2 - a_2b_1)m_C^*}$, are eigenvalues of $D_0(\lambda)$, and $\lambda = 0$ is a simple eigenvalue for $D_{n^*}(\lambda)$, with other eigenvalues having negative real parts. Then, by straightforward calculations, we have

$$\begin{aligned} \phi_1 &= \begin{pmatrix} 1 \\ \frac{d_1\mu_{n^*} - a_1}{a_2} \end{pmatrix}, \quad \psi_1 = \begin{pmatrix} \frac{m_C^*b_1a_2}{(d_1\mu_{n^*} - a_1)^2 + m_C^*b_1a_2} \\ \frac{a_2(d_1\mu_{n^*} - a_1)}{(d_1\mu_{n^*} - a_1)^2 + m_C^*b_1a_2} \end{pmatrix}^T, \\ \phi_2 &= \begin{pmatrix} 1 \\ \frac{i\omega - a_1}{a_2} \end{pmatrix}, \quad \psi_2 = \begin{pmatrix} \frac{a_2m_C^*b_1}{(i\omega - a_1)^2 + a_2m_C^*b_1} \\ \frac{a_2(i\omega - a_1)}{(i\omega - a_1)^2 + a_2m_C^*b_1} \end{pmatrix}^T. \end{aligned}$$

Therefore, $\Phi = (\phi_1, \phi_2, \bar{\phi}_2)$ and $\Psi = (\psi_1, \psi_2, \bar{\psi}_2)^T$ satisfying $\Phi\Psi = I_3$, where I_3 is the identity matrix. By [15], we can compute the following parameters.

$$\begin{aligned} a_1(\sigma) &= \frac{1}{2}\psi_1(L_1(\sigma)\phi_1 - \mu_{n^*}D_1(\sigma)\phi_1), \\ a_{200} &= a_{011} = b_{110} = 0, \\ b_2(\sigma) &= \frac{1}{2}\psi_2(L_1(\sigma)\phi_2 - 0D_1(\sigma)\phi_2), \\ a_{300} &= \frac{1}{4}\psi_1C_{\phi_1\phi_1\phi_1} + \frac{1}{\omega}\psi_1Re[iQ_{\phi_1\phi_2}\psi_2]Q_{\phi_1\phi_1} + \psi_1Q_{\phi_1(h_{200}^0 + \frac{1}{\sqrt{2}}h_{200}^{2n^*})}, \\ a_{111} &= \psi_1C_{\phi_1\phi_2\bar{\phi}_2} + \frac{2}{\omega}\psi_1Re[iQ_{\phi_1\phi_2}\psi_2]Q_{\phi_2\bar{\phi}_2} + \psi_1(Q_{\phi_1(h_{011}^0 + \frac{1}{\sqrt{2}}h_{011}^{2n^*})} + Q_{\phi_2h_{101}^{n^*}} \\ &\quad + Q_{\bar{\phi}_2h_{110}^{n^*}}), \\ b_{210} &= \frac{1}{2}\psi_2C_{\phi_1\phi_1\phi_2} + \frac{1}{2i\omega}\psi_2(2Q_{\phi_1\phi_1}\psi_1Q_{\phi_1\phi_2} + (-Q_{\phi_2\phi_2}\psi_2 + Q_{\phi_2\bar{\phi}_2}\bar{\psi}_2)Q_{\phi_1\phi_1}) \\ &\quad + \psi_2(Q_{\phi_1h_{110}^{n^*}} + Q_{\phi_2h_{200}^0}), \\ b_{021} &= \frac{1}{2}\psi_2C_{\phi_2\phi_2\bar{\phi}_2} + \frac{1}{4i\omega}\psi_2\left(\frac{2}{3}Q_{\bar{\phi}_2\bar{\phi}_2}\bar{\psi}_2Q_{\phi_2\phi_2} + (-2Q_{\phi_2\phi_2}\psi_2 + 4Q_{\phi_2\bar{\phi}_2}\bar{\psi}_2)Q_{\phi_2\bar{\phi}_2}\right) \\ &\quad + \psi_2(Q_{\phi_2h_{011}^0} + Q_{\bar{\phi}_2h_{020}^0}), \end{aligned}$$

where

$$\begin{aligned} h_{200}^0 &= -\frac{1}{2}L^{-1}(0)Q_{\phi_1\phi_1} + \frac{1}{2\omega i}(\phi_2\psi_2 - \bar{\phi}_2\bar{\psi}_2)Q_{\phi_1\phi_1}, \\ h_{200}^{2n^*} &= -\frac{1}{2\sqrt{2}}[L(0) - 4\mu_{n^*}D(0)]^{-1}Q_{\phi_1\phi_1}, \\ h_{011}^0 &= -L^{-1}(0)Q_{\phi_2\bar{\phi}_2} + \frac{1}{\omega i}(\phi_2\psi_2 - \bar{\phi}_2\bar{\psi}_2)Q_{\phi_2\bar{\phi}_2}, \end{aligned}$$

$$\begin{aligned}
 h_{020}^0 &= \frac{1}{2}[2i\omega I - L(0)]^{-1}Q_{\phi_2\phi_2} - \frac{1}{2\omega i}\left(\phi_2\psi_2 + \frac{1}{3}\bar{\phi}_2\bar{\psi}_2\right)Q_{\phi_2\phi_2}, \\
 h_{110}^{n_*} &= [i\omega I - (L(0) - \text{diag}(-\mu_{n_*}, -d_{n_*}\mu_{n_*}))]^{-1}Q_{\phi_1\phi_2} - \frac{1}{\omega i}\phi_1\psi_1Q_{\phi_1\phi_2}, \\
 h_{002}^0 &= \overline{h_{020}^0}, \quad h_{101}^{n_*} = \overline{h_{110}^{n_*}}, \quad h_{011}^{2n_*} = 0.
 \end{aligned}$$

According to [15], the normal form restricted to the third order on the central manifold of the reaction-diffusion system (1.2) at the Turing-Hopf singularity is

$$\begin{cases} \dot{z}_1 = a_1(\sigma)z_1 + a_{200}z_1^2 + a_{011}z_2\bar{z}_2 + a_{300}z_1^3 + a_{111}z_1z_2\bar{z}_2 + o(|z|^4), \\ \dot{z}_2 = i\omega z_2 + b_2(\sigma)z_2 + b_{110}z_1z_2 + b_{210}z_1^2z_2 + b_{021}z_2^2\bar{z}_2 + o(|z|^4), \\ \dot{\bar{z}}_2 = -i\omega\bar{z}_2 + \bar{b}_2(\sigma)\bar{z}_2 + \bar{b}_{110}z_1\bar{z}_2 + \bar{b}_{210}z_1^2\bar{z}_2 + \bar{b}_{021}z_2\bar{z}_2^2 + o(|z|^4). \end{cases} \tag{4.3}$$

Through the parameter transformation $z_1 = r$, $z_2 = \rho\cos\theta - i\rho\sin\theta$, the normal form Eq.(4.3) can be rewritten into real coordinates form (the third-order term is truncated and the azimuth angle is removed item θ)

$$\begin{cases} \dot{r} = a_1(\sigma)r + a_{300}r^3 + a_{111}r\rho^2, \\ \dot{\rho} = \text{Re}(b_2(\sigma))\rho + \text{Re}(b_{210})\rho r^2 + \text{Re}(b_{021})\rho^3. \end{cases} \tag{4.4}$$

5. Numerical simulations

In this section, we perform the numerical simulations. Taking $r = 0.25, K = 14.95, a_{CR} = 1.01, Th_{CR} = 1, \alpha = 2.61, \beta = 0.61, d_1 = 0.01, l = 1$, we have

$$\begin{cases} \frac{\partial u}{\partial t} = 0.01\frac{\partial^2 u}{\partial x^2} + 0.25u\left(1 - \frac{u}{14.95}\right) - \frac{1.01uv}{1 + 1.01u}, \\ \frac{\partial v}{\partial t} = d_2\frac{\partial^2 v}{\partial x^2} + m_C v\left(\frac{2.61 * 1.01u}{1 + 1.01u} - 1 - 0.61v\right). \end{cases} \tag{5.1}$$

Through calculation, we get the unique positive equilibrium point $E_*(u_*, v_*) \approx (0.9483, 0.4539)$. And $a_1 \approx 0.0987, a_2 \approx -0.4892, b_1 \approx 0.3121, b_2 \approx -0.2769$, then hypothesis (A_2) holds. In addition, $S = \{1, 2, 3\}, m_C^* \approx 0.3565, n_* = 2, d_2^{n_*} \approx 0.2072$.

$$\mathcal{H}_0 : m_C = m_C^* \approx 0.3565,$$

is the Hopf bifurcation curve in $m_C - d_2$ plane.

$$\mathcal{L}_n : d_2^n = m_C \left(\frac{b_2d_1\mu_n + (a_2b_1 - a_1b_2)}{\mu_n(-a_1 + d_1\mu_n)} \right), n \in S,$$

are the Turing bifurcation curves. Then, the normal form restricted on center manifold for the reaction-diffusion system (5.1) at Turing-Hopf singularity is

$$\begin{cases} \dot{z}_1 = (-0.1571\sigma_1 + 0.2702\sigma_2)z_1 - 0.0229z_1^3 + 0.0304z_1z_2\bar{z}_2 + o(|z|^4), \\ \dot{z}_2 = 0.2114iz_2 + (-0.1384 + 0.2965i)\sigma_1z_2 - (0.0374 + 0.0395i)z_1^2z_2 \\ \quad - (0.0185 + 0.0824i)z_2^2\bar{z}_2 + o(|z|^4), \\ \dot{\bar{z}}_2 = -0.2114i\bar{z}_2 + (-0.1384 - 0.2965i)\sigma_1\bar{z}_2 - (0.0374 - 0.0395i)z_1^2\bar{z}_2 \\ \quad - (0.0185 - 0.0824i)z_2\bar{z}_2^2 + o(|z|^4). \end{cases}$$

Then we have

$$\begin{cases} \dot{r} = (-0.1571\sigma_1 + 0.2702\sigma_2)r - 0.0229r^3 + 0.0304r\rho^2, \\ \dot{\rho} = -0.1384\sigma_1\rho - 0.0374\rho r^2 - 0.0185\rho^3. \end{cases} \quad (5.2)$$

Considering $\rho > 0$, from [15], the system (5.2) has the following equilibrium points

$$\begin{aligned} A_0 &= (0, 0), \\ A_1^\pm &= (\pm\sqrt{-6.8495\sigma_1 + 11.7833\sigma_2}, 0), \text{ for } -6.8495\sigma_1 + 11.7833\sigma_2 > 0, \\ A_2 &= (0, \sqrt{-7.5000\sigma_1}), \text{ for } \sigma_1 < 0, \\ A_3^\pm &= (\pm\sqrt{-4.5543\sigma_1 + 3.1950\sigma_2}, \sqrt{1.7306\sigma_1 - 6.4757\sigma_2}), \\ &\text{for } -4.5543\sigma_1 + 3.1950\sigma_2 > 0 \text{ and } 1.7306\sigma_1 - 6.4757\sigma_2 > 0. \end{aligned}$$

By [15], we know:

- A_0 is the coexistence equilibrium;
- A_1^\pm are spatially inhomogeneous steady states;
- A_2 is spatially homogeneous periodic solution;
- A_3^\pm are spatially inhomogeneous periodic solutions.

Then, the following critical bifurcation curves can be obtained.

$$\begin{aligned} \mathcal{H}_0 &: \sigma_1 = 0, \\ \mathcal{T} &: \sigma_2 = 0.5813\sigma_1, \\ \mathcal{T}_1 &: \sigma_2 = 1.4254\sigma_1, \sigma_1 \leq 0, \\ \mathcal{T}_2 &: \sigma_2 = 0.2672\sigma_1, \sigma_1 \leq 0. \end{aligned}$$

From Figure 3, it can be seen that the first intersection of the Turing curves \mathcal{L}_n and the Hopf curve \mathcal{H}_0 with $(m_C, d_2) = (m_C^*, d_2^{n*})$ is chosen as the Turing-Hopf bifurcation point. Therefore, the system (5.1) undergoes the Turing-Hopf bifurcation at the point $(m_C^*, d_2^{n*}) = (0.3565, 0.2072)$. Then, the parameter plane partition diagram and phase diagram can be obtained, as shown in Figure 4.

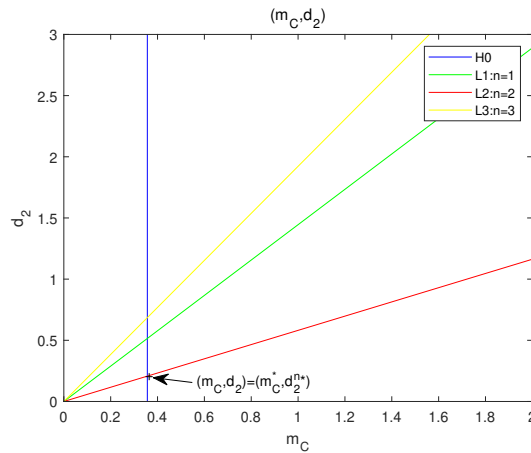


Figure 3. Turing-Hopf bifurcation point (m_C^*, d_2^{n*}) in $m_C - d_2$ plane.

After analysis, for each area, we come to the following conclusions.

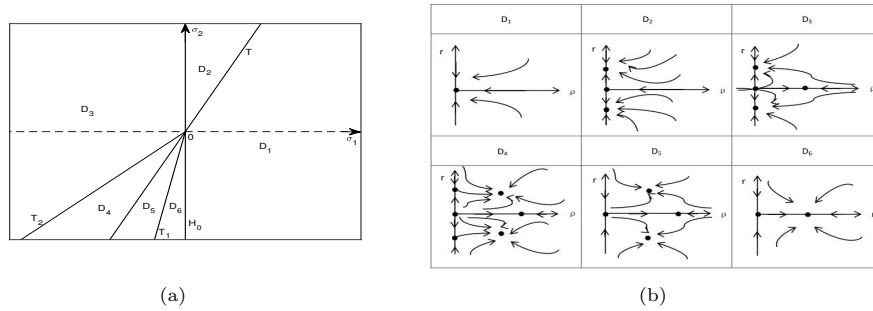


Figure 4. The bifurcation set (a) and the phase portraits (b) for Turing-Hopf bifurcation of the system (5.1).

Proposition 5.1. For given $r = 0.25$, $K = 14.95$, $a_{CR} = 1.01$, $Th_{CR} = 1$, $\alpha = 2.61$, $\beta = 0.61$, $d_1 = 0.01$, $l = 1$, the bifurcation curves \mathcal{H}_0 , \mathcal{T} , \mathcal{T}_1 , \mathcal{T}_2 divide the parameter plane σ_1 - σ_2 into six regions D_1 - D_6 . For each region, different dynamic phenomenon are generated by the system (1.2). The following results can be obtained.

- (1) When $(\sigma_1, \sigma_2) \in D_1$, the system (1.2) has a locally asymptotically stable positive equilibrium point $E_*(u_*, v_*)$ (see Figure 5). Conversely, when $(\sigma_1, \sigma_2) \notin D_1$, the positive equilibrium point $E_*(u_*, v_*)$ becomes unstable.
- (2) When $(\sigma_1, \sigma_2) \in D_2$, the system (1.2) has a pair of stable spatially inhomogeneous steady states (see Figure 6). The spatial patterns and bistability are shown by the system (1.2).
- (3) When $(\sigma_1, \sigma_2) \in D_3$, there is a pair of stable spatially inhomogeneous steady states and an unstable spatially homogeneous periodic solution for the system (1.2) (see Figure 7).
- (4) When $(\sigma_1, \sigma_2) \in D_4$, there is a pair of stable spatially inhomogeneous periodic solutions, a pair of unstable spatially inhomogeneous steady states and an unstable spatially homogeneous periodic solution (see Figure 8).
- (5) When $(\sigma_1, \sigma_2) \in D_5$, there is a pair of stable spatially inhomogeneous periodic solutions and an unstable spatially homogeneous periodic solution (see Figure 10).
- (6) When $(\sigma_1, \sigma_2) \in D_6$, the system (1.2) has a stable spatially homogeneous periodic solution (see Figure 12).

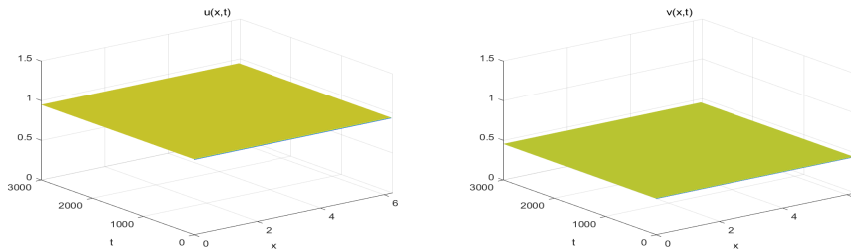
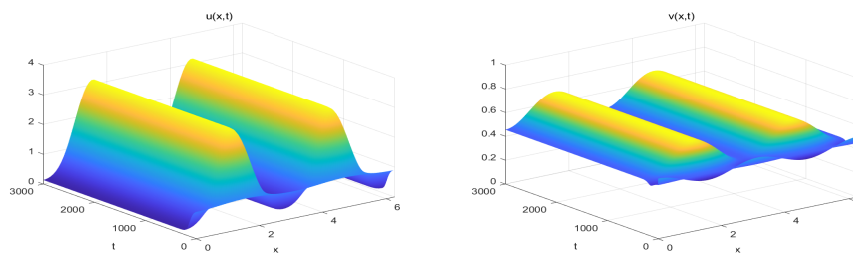
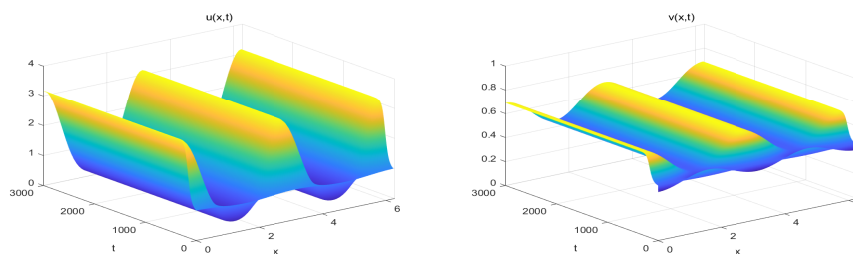


Figure 5. When $(\sigma_1, \sigma_2) = (1, 0)$ lies in region D_1 , the positive equilibrium point $E_*(u_*, v_*) = (0.9483, 0.4539)$ is asymptotically stable and $u(x, 0) = 0.94$, $v(x, 0) = 0.45$ is the initial value.

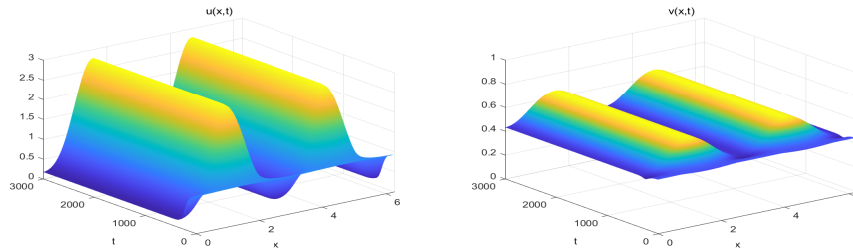


(a) The initial value is $u(x, 0) = 0.948292462 - 0.05\cos(2x), v(x, 0) = 0.453859373 + 0.05\cos(2x)$.

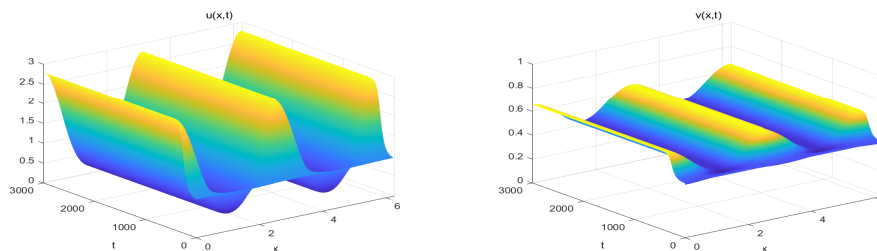


(b) The initial value is $u(x, 0) = 0.948292462 + 0.05\cos(2x), v(x, 0) = 0.453859373 - 0.05\cos(2x)$.

Figure 6. When $(\sigma_1, \sigma_2) = (1, 1)$ lies in region D_2 , the positive equilibrium point $E_*(u_*, v_*) = (0.9483, 0.4539)$ is unstable and there are two stable spatially inhomogeneous steady states like $\cos(2x)$.



(a) The initial value is $u(x, 0) = 0.948292462 - 0.01\cos(2x), v(x, 0) = 0.453859373 + 0.01\cos(2x)$.



(b) The initial value is $u(x, 0) = 0.948292462 + 0.01\cos(2x), v(x, 0) = 0.453859373 - 0.01\cos(2x)$.

Figure 7. When $(\sigma_1, \sigma_2) = (-0.1, 0)$ lies in region D_3 , the positive equilibrium point $E_*(u_*, v_*) = (0.9483, 0.4539)$ is unstable and there are two stable spatially inhomogeneous steady states like $\cos(2x)$.

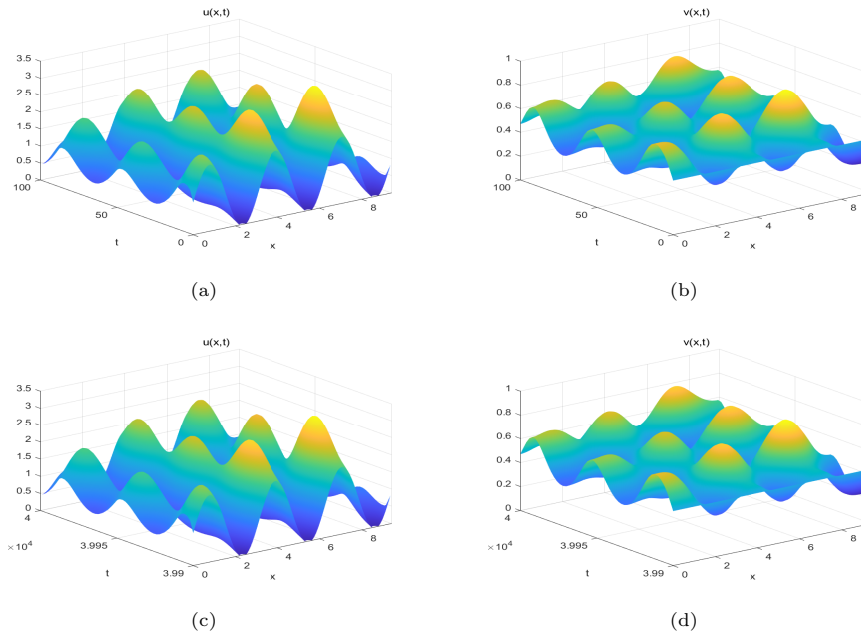


Figure 8. When $(\sigma_1, \sigma_2) = (-0.1, -0.04)$ lies in region D_4 , the positive equilibrium point $E_*(u_*, v_*) = (0.9483, 0.4539)$ is unstable and there are stable spatially inhomogeneous periodic solutions. The initial value is $u(x, 0) = 0.948292462 + \sin(2x)$, $v(x, 0) = 0.453859373$. (a) and (b) are transient behaviours for u and v , respectively; (c) and (d) are long-term behaviours for u and v , respectively.

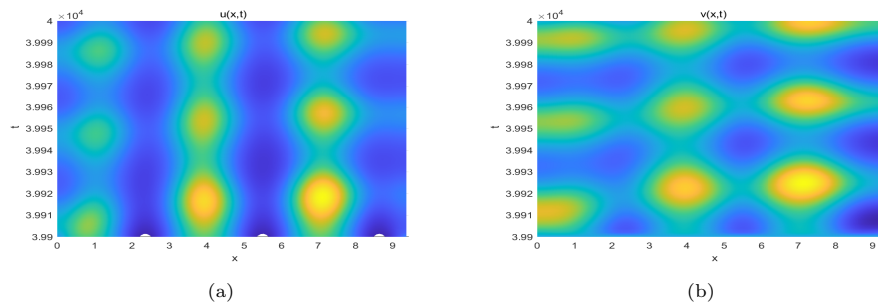


Figure 9. (a) and (b) are the projections of Fig.8 (c) and (d) in the $x - t$ plane, respectively.

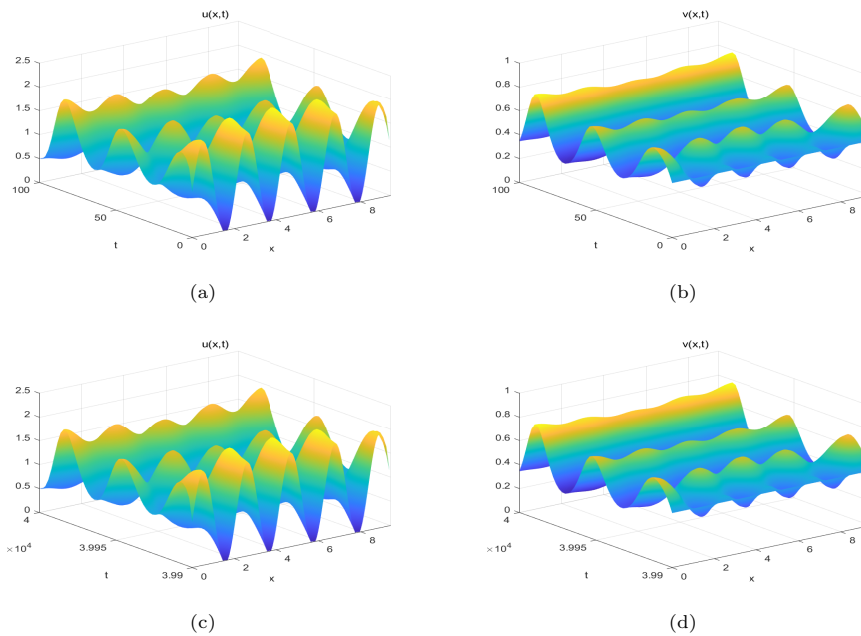


Figure 10. When $(\sigma_1, \sigma_2) = (-0.1, -0.1)$ lies in region D_5 , the positive equilibrium point $E_*(u_*, v_*) = (0.9483, 0.4539)$ is unstable and there are stable spatially inhomogeneous periodic solutions. The initial value is $u(x, 0) = 0.948292462 + \sin(3x)$, $v(x, 0) = 0.453859373$. (a) and (b) are transient behaviours for u and v , respectively; (c) and (d) are long-term behaviours for u and v , respectively.

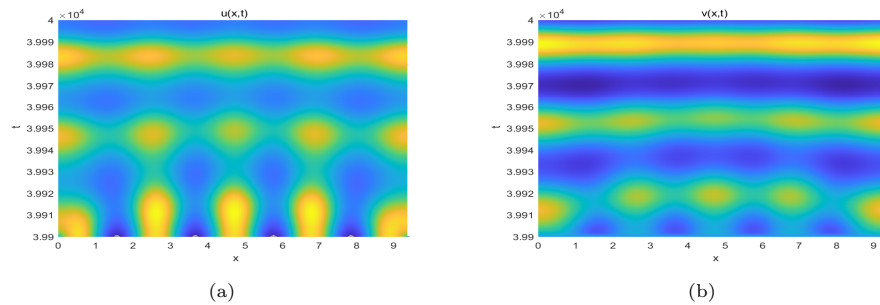


Figure 11. (a) and (b) are the projections of Fig.10 (c) and (d) in the $x - t$ plane, respectively.

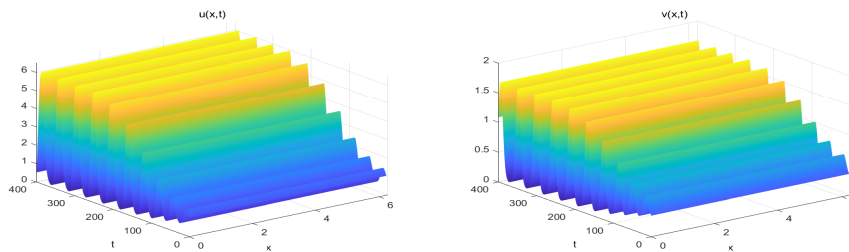


Figure 12. When $(\sigma_1, \sigma_2) = (-0.1, -0.2)$ lies in region D_6 , the positive equilibrium point $E_*(u_*, v_*) = (0.9483, 0.4539)$ is unstable and there is a stable spatially homogeneous periodic solution. The initial value is $u(x, 0) = 0.948292462 + 0.1$, $v(x, 0) = 0.453859373 - 0.1$.

6. Conclusions

In this paper, we consider a diffusive predator-prey model with Holling II functional response. We obtain many interesting results. Mathematically, we analyze the existence and stability conditions for all feasible equilibrium points of the model, and give conditions for the existence of the Turing instability, the Hopf bifurcation and the Turing-Hopf bifurcation, by selecting d_2 and m_C as the Turing and Hopf bifurcation parameters, respectively. We also give the conditions required for the steady-state hydra effects to be able to occur (Theorem 3.2). In addition, we calculate the normal form for the Turing-Hopf bifurcation of the system (1.2) and divide the parameter plane σ_1 - σ_2 into six regions D_1 - D_6 . We analyze each region and find that the system exhibits different spatio-temporal dynamics in different regions, such as spatially non-homogeneous steady-state solutions, spatially homogeneous periodic solutions, and spatially non-homogeneous periodic solutions. Ecologically, the ecological theory obtained in this study may be useful for conservation policy and ecological balance management. In the steady state, the hydra effect can be made to occur in the population by regulating a_1 to achieve the purpose of increasing the predator population size. In addition, predator population size can be improved by adjusting the spatial distribution of predators. Finally, according to the increase of different small perturbations to the predator mortality can make the predator and prey populations exhibit different equilibrium states to improve the corresponding population size to achieve the ideal population size stability state.

References

- [1] P. A. Abrams and C. Quince, *The impact of mortality on predator population size and stability in systems with stage-structured prey*, Theor. Popul. Biol., 2005, 68(4), 253–266.
- [2] P. A. Abrams, *What are hydra effects? A response to Schroder et al.*, Trends Ecol. Evol., 2015, 30(4), 179–180.
- [3] P. D. Adhikary, S. Mukherjee and B. Ghosh, *Bifurcations and hydra effects in Bazykin's predator-prey model*, Theor. Popul. Biol., 2021, 140, 44–53.
- [4] L. D. Anjos, M. I. D. Costa and R. C. Almeida, *Characterizing the existence of hydra effect in spatial predator-prey models and the influence of functional response types and species dispersal*, Ecol. Model., 2020, 428, 109109.
- [5] N. Bajeux and B. Ghosh, *Stability switching and hydra effect in a predator-prey metapopulation model*, Biosystems, 2021, 198.
- [6] M. H. Cortez and P. A. Abrams, *Hydra effects in stable communities and their implications for system dynamics*, Ecology, 2016, 97(5), 1135–1145.
- [7] X. Cao and W. Jiang, *Turing-Hopf bifurcation and spatiotemporal patterns in a diffusive predator-prey system with Crowley-Martin functional response*, Nonlinear Anal. Real World Appl., 2018, 43, 428–450.
- [8] M. H. Cortez and M. Yamamichi, *How (co)evolution alters predator responses to increased mortality: extinction thresholds and hydra effects*, Ecology, 2019, 100(10).
- [9] M. I. D. Costa and L. D. Anjos, *Multiple hydra effect in a predator-prey model*

- with Allee effect and mutual interference in the predator, *Ecol. Model.*, 2018, 373, 22–24.
- [10] H. Chen and C. Zhang, *Analysis of the dynamics of a predator-prey model with Holling functional response*, *JNMA*, 2022, 4(2), 310–324.
- [11] M. H. Cortez, *Hydra effects in discrete-time models of stable communities*, *J. Theor. Biol.*, 2017, 411, 59–67.
- [12] D. L. DeAngelis and S. Yurek, *Spatially explicit modeling in ecology: a review*, *Ecosystems*, 2017, 20(2), 284–300.
- [13] K. Garain and P. S. Mandal, *Bubbling and hydra effect in a population system with Allee effect*, *Ecol. Complex*, 2021, 47, 100939.
- [14] B. Ghosh, O. L. Zhdanova, B. Barman and E. Y. Frisman, *Dynamics of stage-structure predator-prey systems under density-dependent effect and mortality*, *Ecol. Complex*, 2020, 41, 100812.
- [15] W. Jiang, Q. An and J. Shi, *Formulation of the normal form of Turing-Hopf bifurcation in partial functional differential equations*, *J. Differ. Equ.*, 2020, 268(10), 6067–6102.
- [16] Z. Liu and R. Yang, *Hopf bifurcation analysis of a Host-generalist parasitoid model with diffusion term and time delay*, *JNMA*, 2021, 3(3), 447–463.
- [17] K. M. McIntire and S. A. Juliano, *How can mortality increase population size? A test of two mechanistic hypotheses*, *Ecology*, 2018, 99(7), 1660–1670.
- [18] D. Pal, B. Ghosh and T. K. Kar, *Hydra effects in stable food chain models*, *Biosystems*, 2019, 185, 104018.
- [19] C. Qin, J. Du and Y. Hui, *Dynamical behavior of a stochastic predator-prey model with Holling-type III functional response and infectious predator*, *AIMS Math.*, 2022, 7(5), 7403–7418.
- [20] Y. Song, J. Shi and H. Wang, *Spatiotemporal dynamics of a diffusive consumer-resource model with explicit spatial memory*, *Stud. Appl. Math.*, 2021, 148(1), 373–395.
- [21] Q. Song, R. Yang, C. Zhang and L. Wang, *Bifurcation analysis of a diffusive predator-prey model with Beddington-Deangelis functional response*, *J. Appl. Anal. Comput.*, 2021, 11(2), 920–936.
- [22] Y. Song, T. Zhang and Y. Peng, *Turing-Hopf bifurcation in the reaction-diffusion equations and its applications*, *Commun. Nonlinear Sci. Numer. Simul.*, 2015, 33, 229–258.
- [23] A. Schroder, L. Persson and A. M. D. Roos, *Culling experiments demonstrate size-class specific biomass increases with mortality*, *Proc. Natl. Acad. Sci. USA*, 2009, 106(8), 2671–2676.
- [24] A. Schroder, A. van Leeuwen and T. C. Cameron, *When less is more: positive population-level effects of mortality*, *Trends Ecol. Evol.*, 2014, 29(11), 614–624.
- [25] M. Sieber and F. M. Hilker, *The hydra effect in predator-prey models*, *J. Math. Biol.*, 2012, 64(1–2), 341–360.
- [26] X. Tian and S. Guo, *Spatio-temporal patterns of predator-prey model with Allee effect and constant stocking rate for predator*, *Int. J. Bifurcation Chaos*, 2021, 31(16), 2150249.

-
- [27] R. Wang and W. Zhao, *Extinction and stationary distribution of a stochastic predator-prey model with Holling II functional response and stage structure of prey*, J. Appl. Anal. Comput., 2022, 12(1), 50–68.
- [28] L. Wang, C. Dai and M. Zhao, *Hopf bifurcation in an age-structured prey-predator model with Holling III response function*, Math. Biosci. Eng., 2021, 18(4), 3144–3159.
- [29] V. Weide, M. C. Varriale and F. M. Hilker, *Hydra effect and paradox of enrichment in discrete-time predator-prey models*, Math. Biosci., 2019, 317.
- [30] Y. Zhou, X. Yan and C. Zhang, *Turing patterns induced by self-diffusion in a predator-prey model with schooling behavior in predator and prey*, Nonlinear Dyn., 2021, 105(4), 3731–3747.